Simplified Alamouti-Type Space-Time Coding for Image Sensor Communication Using Rotary LED Transmitter

Zhengqiang Tang, *Graduate Student Member, IEEE*, Shintaro Arai, *Member, IEEE*, and Takaya Yamazato, *Senior Member, IEEE*

***Abstract*—This study proposes a simplified Alamouti-type space-time coding (STC), improving the performance of image sensor communication (ISC) using a rotary LED transmitter. The rotary LED transmitter was developed to increase the data rate of ISC using afterimages of LED lights. The transmitter simultaneously causes the LEDs to blink and rotates them around a vertical axis. Owing to the movement of the blinking LEDs that occurs within the exposure time of the camera, multiple blinking states are captured as afterimages, thus increasing the amount of information that can be received per image. However, with increasing communication distance, the size of the LED light captured on the image sensor decreases. In this case, it is difficult to distinguish each LED blinking state, leading to a degradation of the demodulation performance. To overcome this problem, the proposed STC encodes adjacent angular afterimages as symbol pairs and transmits these symbol pairs using two symbol times. In addition, we simplified the data decoding process by using normalized LED luminance values. We evaluate the demodulation performance of the proposed method through experiments. Compared with conventional coding methods, the proposed STC requires no channel estimation and significantly improves the demodulation performance.**

***Index Terms*—Visible light communication, image sensor communication, rotary LED transmitter, afterimages, space-time coding.**

I. Introduction

VISIBLE light communication (VLC) [1] is a method of optical wireless communication [2] according to which information is transferred using visible light. In VLC, LEDs are usually used to transfer optical signals while providing lighting service. As a semiconductor device, the blinking of an LED can be modulated at a frequency exceeding 1 GHz [3]. Therefore, when an LED transfers data in VLC systems, the human eye cannot detect its blinking.

Manuscript received November 9, 2021; revised December 12, 2021; accepted December 17, 2021. Date of publication December 23, 2021; date of current version January 3, 2022. This work was supported in part by JSPS KAKENHI under Grants JP17K18282 and JP21K11948, in part by the joint research program of the Institute of Materials and Systems for Sustainability, Nagoya University, and in part by Nagoya University Interdisciplinary Frontier Fellowship. *(Corresponding author: Zhengqiang Tang.)*

Zhengqiang Tang and Takaya Yamazato are with the Nagoya University, Nagoya-shi 464-8603, Japan (e-mail: tang@katayama.nuee.nagoya-u.ac.jp; yamazato@nagoya-u.jp).

Shintaro Arai is with the Okayama University of Science, Okayama 700-0005, Japan (e-mail: arai@ee.ous.ac.jp).

Digital Object Identifier 10.1109/JPHOT.2021.3137601

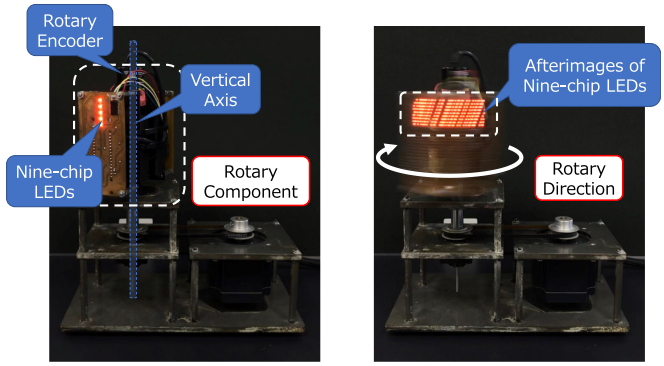

(a) The structure of the transmitter. (b) The state of rotating.

Fig. 1. Rotary LED transmitter.

In this paper, we focus on VLC using an image sensor (camera) as a receiver, which is commonly referred to as image sensor communication (ISC) [4], [5] or optical camera communication. In ISC, the receiver camera captures the blinking states of the LEDs and outputs them as an image [6]. Because the data are demodulated from a two-dimensional (2D) image, an image processing technique can spatially separate the signal and non-signal light sources. This means that ISC is largely immune to noise [7]–[9]. However, the speed of ISC is basically determined by the shooting speed of the camera. To achieve high communication speeds, some studies have employed high-speed cameras as receivers [10], [11]. Unfortunately, commercial cameras capture tens of frames per second. If a transmitter LED is modulated by ON–OFF keying (OOK), the commercial camera receives only tens of bits per second (bps), which does not lead to a satisfying communication speed. Therefore, improving the communication speed when using commercial cameras is a major challenge in ISC [12], [13]. In our previous studies, we developed a *rotary LED transmitter* to solve this issue [14], [15]. The rotary LED transmitter is shown in Fig. 1. This transmitter rotates the rotary component and switches the blinking states of the LEDs. The relative movement between the LEDs and the camera produces an afterimage, in which the change in the LED blinking states is recorded. By using the afterimage, the amount of information received per image can be increased, thereby

improving the speed of ISC. A detailed description of the structure of the transmitter and the mechanism of the data transmission rate improvement have been provided in [15]. In this study, we especially focus on the demodulation performance of ISC using the rotary LED transmitter and propose a space-time coding (STC) method to improve its communication quality.

The purpose of this paper is to improve the demodulation performance of ISC using a rotary LED transmitter. The size of the LED light captured in the image shrinks as the communication distance grows, as does the interval between adjacent afterimages [15]. This makes the distinction between the LED blinking states difficult, negatively affecting the communication quality. In 2013, Amano *et al.* proposed an STC method, which is based on the principle proposed by Alamouti in 1998 [16], to expand the communication range for conventional ISC system [17]. In this study, we particularly propose a simplified Alamouti-type STC for the ISC using a rotary LED transmitter. According to the proposed method, the afterimages of adjacent angles in the direction of rotation are assembled into symbol pairs, and we transmit the symbol pairs using two symbol times. The receiver first normalizes the received LED luminance values, then uses two pixels to demodulate the transmitted data from two captured images. Thanks to the normalization operation, the estimation of the channel coefficient is not necessary. According to the communication distance, the Alamouti-type STC is divided into two approaches: short-distance STC and long-distance STC. Short-distance STC is used if two neighboring lights of LEDs can be separated at the image plane, otherwise, long-distance STC is used. Due to the cylindrical rotation of the rotary LED transmitter, LED lights overlap on both sides of the captured image, in which the blinking states are difficult to distinguish. To avoid this problem, the data transmission angular range of the rotary LED transmitter was set to a fixed range from the center of the captured image [15]. The fixed data transmission angular range ensures the interval between neighboring afterimages of LED lights, therefore the blinking states of LED lights are separable. In this case, we believe that the effect of long-distance STC will not be significant, so we choose short-distance STC to improve the demodulation performance in this study. The proposed method counters light interference and background noise by modulating the signals with respect to both space (i.e., rotation) and time. In this way, we enhance the reliability of the transmitting signals, improving the demodulation performance. In this study, we evaluate the demodulation performance of the proposed method by experiments.

II. ISC System Using Rotary LED Transmitter

A block diagram of the proposed ISC system is illustrated in Fig. 2. The rotary LED transmitter cylindrically rotates the nine-chip LEDs and switches the blinking state every $\Delta\theta$ degrees of rotation. In this study, we set $\Delta\theta$ to 1°. The proposed Alamouti-type STC was chosen as the modulation method. The blinking state of each LED is controlled by a rotary encoder, a microcomputer, and an LED driver. The rotary encoder outputs a clock signal every 1° of rotation. Then, the microcomputer

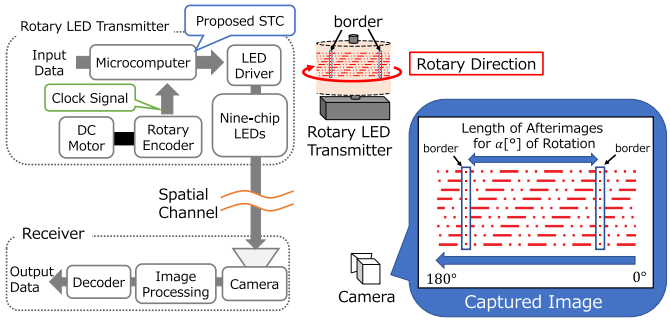

Fig. 2. System model of the ISC using a rotary LED transmitter.

assigns modulated data to each LED via the LED driver in response to the clock signal. We set the angular range of the data transmission to α degrees. To identify the angular range, all LEDs switch to the ON state every α degrees. In this study, we call the blinking pattern in which all the LEDs are in the ON state a "*border*."

The receiver is composed of a commercial camera, an image processing unit, and a decoder. The camera captures the LED lights and converts them into electrical signals to be output as an image. Then, we detect the position of each LED in the captured image and extract its luminance value as a pixel via image processing. Finally, the decoder demodulates the data with the extracted pixel according to the decoding method of STC.

Here, we compare the proposed ISC system with a conventional ISC system using a large array-type transmitter in terms of cost, complexity, and reliability. Because the proposed system receives $9 \times \alpha$ afterimages of LED lights per image, we assume that the conventional system uses an array-type transmitter with $9 \times \alpha$ LEDs arranged in a matrix. First, we compare the cost and complexity of the rotary LED transmitter versus the LED array transmitter. The number of LEDs the rotary LED transmitter used is 9, whereas that of the LED array transmitter is $9 \times \alpha$. The rotary LED transmitter uses fewer LEDs than the LED array transmitter. Therefore, the cost of LEDs is lower and the complexity of the LED control circuit is simpler compared with the conventional system. On the other hand, the rotary LED transmitter requires a motor to rotate LEDs. This means extra cost in terms of the transmitter mechanism. However, the proposed technique is designed to be attached to rotating devices (e.g., vision displays [18]). In this case, the energy for rotation is provided separately, so the cost of the proposed system can be reduced. Next, we compare the reliability of the two transmitters. The rotary LED transmitter uses the afterimage of LED lights to transmit signal by rotating 9 LEDs during the camera exposure time. This allows the proposed system to transmit more signals with fewer LEDs. As shown in Fig. 1(b), the camera captures blinking states of LEDs as afterimages arranged like an LED array. It is similar to the LED lights obtained by capturing an LED array transmitter. Therefore, we believe that the rotary LED transmitter ensures the same level of reliability as the LED array transmitter.

TABLE I
TRANSMITTING SIGNAL AT EACH ROTATION ANGLE

Symbol Time \ Rotation Angle	$2p$	$2p+1$
Δt_1	s_{2p}	s_{2p+1}
Δt_2	$\overline{s}_{2p+1}$	s_{2p}

III. SIMPLIFIED ALAMOUTI-TYPE STC

A. Encoding Process

Here, we explain the proposed method. We set the data transmission angle to range from 0 to $(\alpha - 1)$ degrees. The rotation angle of the transmitter is represented by p (0, 1, ..., p, ..., $\alpha - 1$). We assembled the afterimages of the $2p$-th degree and the $(2p + 1)$-th degree as a symbol pair. The time period that the transmitter takes to rotate 360° is represented by Δt. Thus, Δt denotes one symbol time period. First, consider Δt_1 and Δt_2 denote the first and second symbol times, respectively. As shown in Table I, in Δt_1, the signal transmitted from the $2p$-th degree is denoted by s_{2p}, and that transmitted from the $(2p + 1)$-th degree is denoted by s_{2p+1}. In Δt_2, we transmit the signal $\overline{s}_{2p+1}$ at the $2p$-th degree and the signal s_{2p} at the $(2p + 1)$-th degree. Here, $\overline{s}_p$ indicates the intensity (luminance) of the inverted signal of s_p, which is calculated as follows:

$$\overline{s}_p = A - s_p, \tag{1}$$

where A indicates the light intensity (luminance value) received by the camera from an LED when it is ON.

The proposed method modulates the transmitting signals with respect to both rotation and time using two adjacent afterimages. The number of adjacent afterimages modulated to transmit the signals is increased every 2^m $(m = 1, 2, 3, \ldots)$. This study only discusses the STC when $m = 1$.

B. Communication Channel Model

As shown in Fig. 3, we assume that the transmitting signals (s) from the $2p$-th and $(2p + 1)$-th degrees pass through a spatial channel and are received by two arbitrary pixels: Pixel$_u$ and Pixel$_v$. Let h_1 and h_2 denote the channel coefficients from the $2p$-th degree and the $(2p + 1)$-th degree to Pixel$_u$, respectively. Then, let h_3 and h_4 denote the channel coefficients from the $2p$-th degree and the $(2p + 1)$-th degree to Pixel$_v$, respectively. Both coefficient h_2 and h_3 indicate the light interference in an assembled symbol pair (i.e., the inter-symbol interference). To be more specific, the coefficient h_2 is the light interference that Pixel$_u$ receives from the $(2p + 1)$-th degree. The coefficient h_3 is the light interference that Pixel$_v$ receives from the $2p$-th degree.

The receiving signal (luminance value) is denoted by r. In Δt_1, the receiving signals at Pixel$_u$ and Pixel$_v$ are denoted by $r_{2p}^{\Delta t_1}$ and $r_{2p+1}^{\Delta t_1}$, respectively. In Δt_2, the receiving signals at Pixel$_u$ and Pixel$_v$ are denoted by $r_{2p}^{\Delta t_2}$ and $r_{2p+1}^{\Delta t_2}$, respectively. Using the property measured by (1), the receiving signals at each pixel can be expressed as follows:

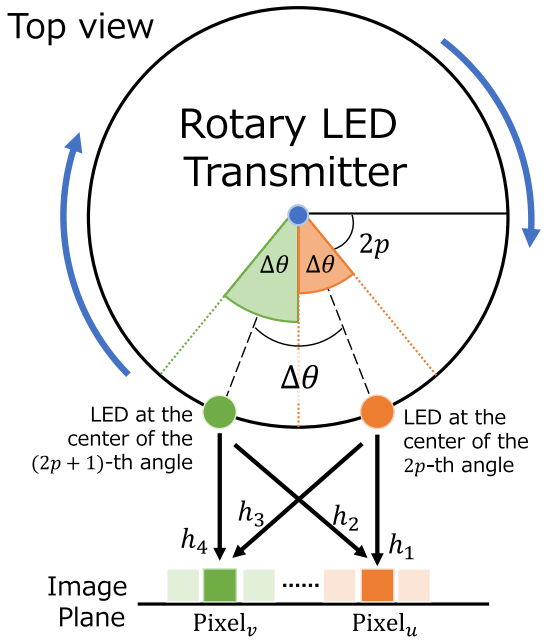

Fig. 3. Communication channel model of the proposed method.

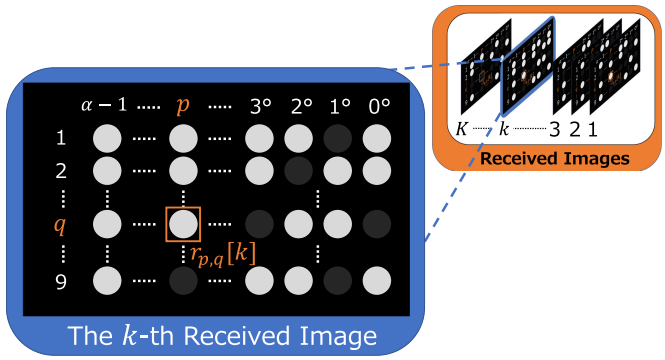

Fig. 4. Normalization for the received LED luminance values.

$$\begin{cases} r_{2p}^{\Delta t_1} = h_1 s_{2p} + h_2 s_{2p+1} + n_1 \\ r_{2p+1}^{\Delta t_1} = h_3 s_{2p} + h_4 s_{2p+1} + n_2 \\ r_{2p}^{\Delta t_2} = h_2 s_{2p} - h_1 s_{2p+1} + h_1 A + n_3 \\ r_{2p+1}^{\Delta t_2} = h_4 s_{2p} - h_3 s_{2p+1} + h_3 A + n_4 \end{cases}, \tag{2}$$

where n_i $(i = 1, 2, 3, 4)$ denotes the noise.

C. Decoding Process

1) Normalization of Received LED Luminance Values: In this study, we normalized the luminance values of the received LEDs before data decoding. Let K denote the total number of received images. Let $r_{p,q}[k]$ denote the received luminance value of the LED in the q-th (0, 1, ..., q, ..., 9) row and at the p-th (0, 1, ..., p, ..., $\alpha - 1$) degree of the k-th (0, 1, ..., k, ..., K) received image, as shown in Fig. 4. Then, let $E_{p,q}$ denote the

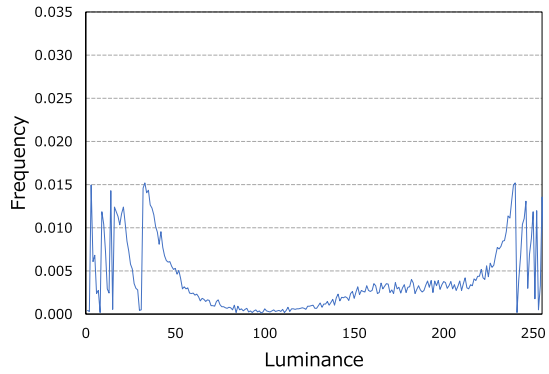

(a) Before the normalization.

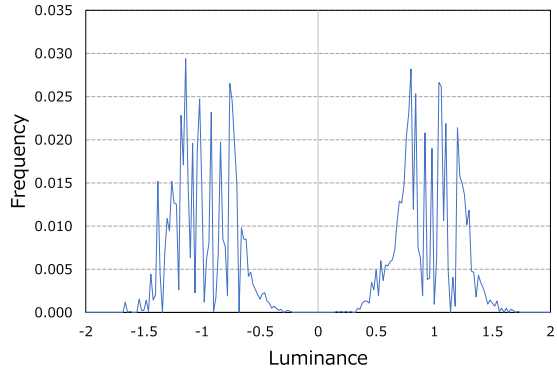

(b) After the normalization.

Fig. 5. The distribution of the received LED luminance values when the communication distance of the experiment is 3.0 m.

mean of $r_{p,q}$, and $E_{p,q}$ is calculated as follows:

$$E_{p,q} = \frac{\sum_{k=1}^{K} r_{p,q}[k]}{K}. \tag{3}$$

Let $V_{p,q}$ denotes the variance of $r_{p,q}$, and $V_{p,q}$ is calculated as follows:

$$V_{p,q} = \frac{\sum_{k=1}^{K} (r_{p,q}[k] - E_{p,q})^2}{K}. \tag{4}$$

The normalized value of $r_{p,q}[k]$ is denoted by $\hat{r}_{p,q}[k]$, and $\hat{r}_{p,q}[k]$ can be calculated as follows:

$$\hat{r}_{p,q}[k] = \frac{r_{p,q}[k] - E_{p,q}}{\sqrt{V_{p,q}}}. \tag{5}$$

The normalized value of received LED luminance ($\hat{r}$) is used to calculate the symbol decision value, which is denoted by $\tilde{s}$. After the normalization process, the value of $h_j A\,(j = 1, 2, 3, 4)$ converges to 0. This means that the estimation of the channel coefficients is not required in our proposed method.

Fig. 5 illustrates the distribution of the received LED luminance values before and after the normalization process in the experiment. As can be seen, the luminance distribution became two peaks after the normalization. In this case, the receiver can easily distinguish the received LED luminance and demodulate the data correctly.

TABLE II
EXPERIMENTAL SPECIFICATIONS

LED	SML-M12UTT86
Number of LEDs (N_L)	9
Switching angle for blinking ($\Delta\theta$)	1°
Date angle range (α)	60°
Rotary speed (S_r)	300 rpm
LED rotating radius	58 mm
Camera	UI-3250ML
Camera resolution	1,600 × 1,200
Focal length of Lens (f)	35 mm
Aperture	F4
Shooting speed	5 fps
Exposure time	0.2 s
Lens filter	ND8
Communication distance (D)	1.0–10.0 m

2) Recovering Data in Short-Distance STC: As described in Section I, we use short-distance STC for our ISC system. When the communication distance is short, there is a large interval between adjacent afterimages on the image sensor, and there are multiple pixels between Pixel$_u$ and Pixel$_v$. In this case, the inter-symbol interference is weak. Therefore, we consider (2) with $h_2 = 0$, $h_3 = 0$, and $h_1 = h_4$. Because $h_j A$ is normalized to 0, the normalized receiving signals can be expressed as follows:

$$\begin{cases} \hat{r}_{2p}^{\Delta t_1} = h_1 s_{2p} + n_1 \\ \hat{r}_{2p+1}^{\Delta t_1} = h_1 s_{2p+1} + n_2 \\ \hat{r}_{2p}^{\Delta t_2} = -h_1 s_{2p+1} + n_3 \\ \hat{r}_{2p+1}^{\Delta t_2} = h_1 s_{2p} + n_4. \end{cases} \tag{6}$$

The symbol decision values $\{\tilde{s}_{2p}, \tilde{s}_{2p+1}\}$ of short-distance STC can be calculated as follows:

$$\begin{cases} \tilde{s}_{2p} = \hat{r}_{2p}^{\Delta t_1} + \hat{r}_{2p+1}^{\Delta t_2} = 2h_1 s_{2p} + n_1 + n_4 \\ \tilde{s}_{2p+1} = \hat{r}_{2p+1}^{\Delta t_1} - \hat{r}_{2p}^{\Delta t_2} = 2h_1 s_{2p+1} + n_2 - n_3 \end{cases}. \tag{7}$$

Finally, we demodulate the data using the calculated $\tilde{s}$. If $\tilde{s}$ is greater than or equal to 0, we demodulate the data as "1." Otherwise, we demodulate the data as "0."

IV. EXPERIMENT

A. Experimental Conditions

In this study, we experimentally evaluate the demodulation performance of the proposed method. The experimental conditions are listed in Table II, and Fig. 6 shows a photograph of the experimental setup. The transmitter blinked nine-chip LEDs every 1° of rotation across the front of the camera lens. We set the angular range of data transmission (α) to 60° and fixed the rotary speed to 300 rotations per minute (rpm). The data were generated by an M-sequence [19] and modulated by the proposed method described in Section III-A. The M-sequence is a pseudo-random binary sequence that can reproduce any binary sequence except

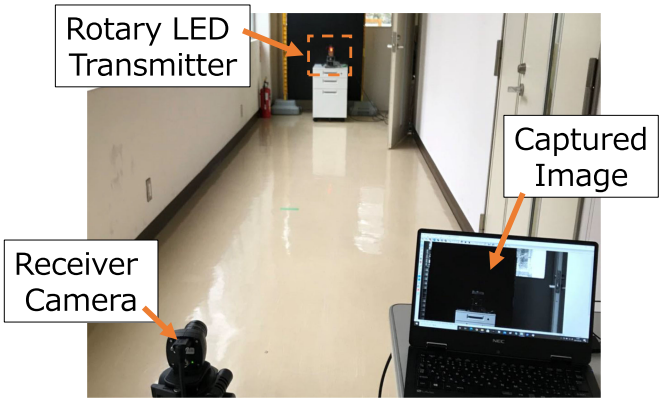

Fig. 6. The experimental scene.

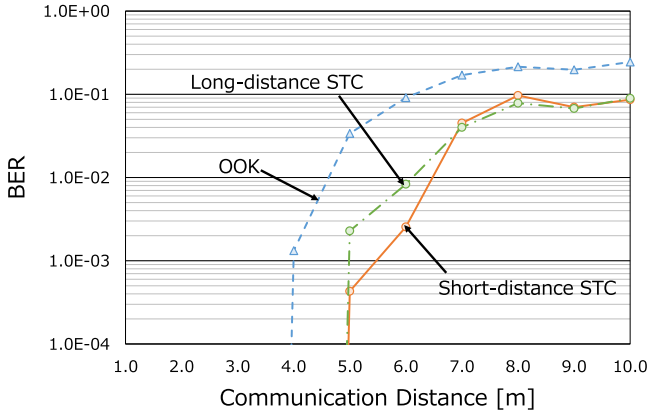

Fig. 7. Demodulation performance versus communication distance. All these methods demodulated the data using normalized luminance values.

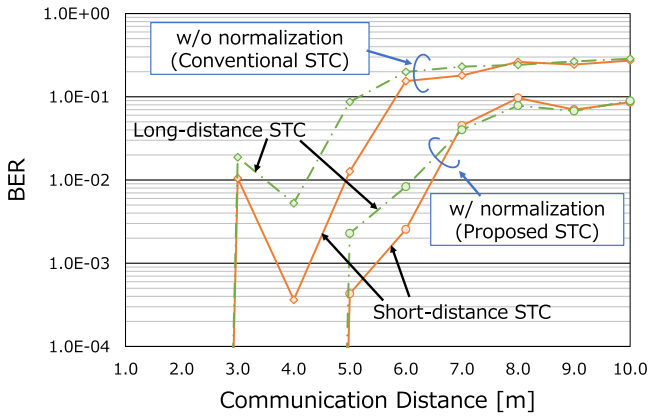

Fig. 8. Comparison of the Alamouti-type STC with and without the normalization operation.

the zero vector. The M-sequence was used to generate random transmitting data in this study. The receiver is never aware that the data being transmitted was generated using the M-sequence. To put it another way, the decoder does not recover data using M-sequence features.

On the receiving side, a complementary metal oxide semiconductor (CMOS) camera was used. We used a camera lens with a focal length of 35 mm and fixed the aperture at F4. We set the shooting speed (frame rate) to 5 frames per second (fps). The camera's exposure time was set to 0.2 seconds which is the same as its shooting time. The resolution of the image sensor (camera) is 1,600 $\times$ 1,200. In addition, we attached an ND8 filter to prevent the saturation of the LED light received by the camera. The coordinates of the captured afterimage of the LED lights and the borders were obtained in advance. In this study, we focus on evaluating the communication performance of the proposed STC.

In our previous study, we modulated the data using OOK and demodulated the data using a threshold decision [15]. For a fair comparison, OOK also demodulated the data using normalized luminance values in this study. The communication distance was set to range from 1.0 to 10.0 m, and we transmitted 30,240 bits of data every 1.0 m and measured the bit error rate (BER). The BER is calculated by counting the number of error bits and dividing it by the total number of bits transmitted.

B. Experimental Result

Now, we discuss the experimental results. Fig. 7 shows the BER versus communication distance. The result of long-distance STC is shown in Fig. 7 as well. As we can see, the proposed STC extended the error-free transmission distance compared with that achieved by OOK. At 5.0 m, the BER of short-distance STC was approximately 4×10^{-4}, whereas that of OOK was greater than 1×10^{-2}. When the communication distance exceeded 7.0 m, the BER of STCs was less than 1×10^{-1}, whereas that of OOK was approximately 2×10^{-1}. These results indicate that the proposed method is able to improve the demodulation performance for our ISC system. This is because the proposed STC achieves diversities with respect to time and space by transmitting signals using two symbol times and recovering data using two pixels. The proposed method counters the impact of the ambient light noise and the interference of other LED lights, thus increasing the robustness of the transmitting signals.

In addition, we found that the difference between the BER of long- and short-distance STC was not significant when communicating over 7.0 m. This indicates that the long-distance STC's effectiveness was not significant which is in line with our prediction in Section I.

To evaluate the effectiveness of the normalization operation, we provide the experimental result of Alamouti-type STC without using the normalized luminance values (conventional STC). The demodulation method of the conventional STC can be referred to [17]. Fig. 8 shows the comparison of demodulation performance of the STC with and without the normalization operation. First, we focus on the BER of the conventional STC. As shown in Fig. 8, the BER of conventional STC at 4.0 m was lower than that at 3.0 m. The phenomenon was caused by the cylindrical rotation motion of the rotary LED transmitter and was influenced by the LED size, the pixel size, the aperture, and the focal length of the camera lens. The reason why this phenomenon occurs has been discussed in [15] in detail. As shown in Fig. 8, the error-free transmission distance of the conventional STC was 3.0 m, whereas that of the Alamouti-type STC with the normalization operation (proposed STC) was 5.0 m. The

TABLE III
DATA TRANSMISSION RATE USING 9 LEDS WHEN THE CAMERA SHOOTING SPEED IS SET TO 5 FPS

	LED array	Rotary LED transmitter
OOK	45 bps	2,700 bps
Proposed STC	22.5 bps	1,350 bps

proposed STC increased the error-free transmission distance by 2.0 m compared to the conventional STC. Furthermore, when the communication distance was less than 7.0 m, the proposed STC outperformed the conventional STC by more than one order of magnitude. The proposed STC improved the demodulation performance of long-distance communications even at distances greater than 7.0 m. This is because the normalization operation splits the distribution of LED luminances into two peaks, increasing the recognition for data demodulation, as described in Section III-C1. These gains in demodulation performance indicate that the normalization operation we included in the decoding process is very effective and important.

In this study, the value of $\Delta\theta$ was set to 1°. The communication performance can be simply improved by physically reducing the resolution of the rotary LED transmitter (e.g., transfer 1 bit of data using 2° of rotation angles). However, we consider $\Delta\theta$ and α as the intrinsic parameters of the rotary LED transmitter. The performance improvement achieved by changing these intrinsic parameters is an inherent capability of the ISC system using a rotary LED transmitter. In contrast, the proposed STC enhances the reliability of the transmitting signals by achieving diversity in space and time. The proposed method can be applied to any resolution of the rotary LED transmitter. In other words, the proposed STC is effective when 2° of rotation angles are used to transmit 1 bit of data as well. To quantitatively evaluate the communication performance for the ISC system using a rotary LED transmitter, setting the intrinsic parameters to constant is necessary.

Finally, we evaluate the data transmission rate for the ISC using a rotary LED transmitter. We listed the data transmission rates in OOK and the proposed STC when an LED array or a rotary LED transmitter is used in Table III. A LED array transmitter refers to a matrix of LEDs [6]. When the camera shooting speed remains constant, the rotary LED transmitter improves communication speed compared to an LED array transmitter with the same number of LEDs. For example. we assume that an LED array transmitter with 9 LEDs transfers signals using OOK. The camera's frame rate is assumed to be 5 fps. The LED array transmitter and the receiver camera are assumed to be fully synchronized. In this case, the data transmission rate using an LED array transmitter is 45 ($= 9 \times 5$) bps. Under the same experimental conditions, the rotary LED transmitter achieves a rate of 2,700 ($= 9 \times 60 \times 5$) bps by using afterimages. That is 60 times the rate using an LED array transmitter. When we change the modulation method, the rotary LED transmitter is capable of improving the communication speed of ISC as well. The details of the data rate improvement by using the rotary LED transmitter can be referred to in [15]. The data transmission rate could be further improved by increasing the rotary speed (S_r), the number of LEDs (N_L), or α, or by reducing $\Delta\theta$.

V. CONCLUSION

In this paper, we proposed a simplified Alamouti-type STC based on afterimages of LED lights for an ISC system using a rotary LED transmitter. The proposed method assembles two signals as a symbol pair and modulates the pair with respect to space and time. Owing to the resulting diversity in space and time, the reliability of the transmitting signals is increased. We also incorporated a normalization method into the decoding process, meaning the proposed method is able to demodulate data without channel estimation. Our experimental results indicate that the proposed method improves the demodulation performance as compared with conventional methods.

In future work, we will explore further improvements in the demodulation performance, especially for long-distance communication. Coding methods such as Manchester code and 4B6B code [20] could improve the demodulation performance for the ISC system as well. We would like to compare these coding methods with the proposed STC in future. Another technique which can be used with a slightly defocused image is the rolling shutter ISC [12]. We also consider comparing the proposed ISC with the rolling shutter ISC eventually.

ACKNOWLEDGMENT

The authors would like to thank Prof. Toshiaki Fujii (Nagoya University), Prof. Hiraku Okada (Nagoya University), Prof. Tomohiro Yendo (Nagaoka University of Technology), Prof. Koji Kamakura (Chiba Institute of Technology), and Dr. Masayuki Kinoshita (Chiba Institute of Technology) for useful discussions and suggestions.

REFERENCES

[1] T. Komine and M. Nakagawa, "Fundamental analysis for visible light communication system using LED lights," *IEEE Trans. Consum. Electron.*, vol. 50, no. 1, pp. 100–107, Feb. 2004.
[2] S. Arai, M. Kinoshita, and T. Yamazato, "Optical wireless communication: A candidate 6G technology?," *IEICE Trans. Fundamentals*, vol. E104-A, no. 1, pp. 227–234, Jan. 2021.
[3] L. Wang *et al.*, "1.3 GHz E-O bandwidth GaN-based micro-LED for multi-gigabit visible light communication," *Photon. Res.*, vol. 9, no. 5, pp. 792–802, May 2021.
[4] H. B. C. Wook, S. Haruyama, and M. Nakagawa, "Visible light communication with LED traffic lights using 2-dimensional image sensor," *IEICE Trans. Fundamentals*, vol. E 89-A, no. 3, pp. 654–659, Mar. 2006.
[5] T. Yamazato *et al.*, "Image-sensor-based visible light communication for automotive applications," *IEEE Commun. Mag.*, vol. 52, no. 7, pp. 88–97, Jul. 2014.
[6] K. Kamakura, "Image sensors meet LEDs," *IEICE Trans. Commun.*, vol. E100-B, no. 6, pp. 917–925, Jun. 2017.
[7] S. Arai, H. Matsushita, Y. Ohira, T. Yendo, D. He, and T. Yamazato, "Maximum likelihood decoding based on pseduo-captured image templates for image sensor communication," *Nonlinear Theory Appl., IEICE*, vol. 10, no. 2, pp. 173–189, Apr. 2019.
[8] Y. Ohira, T. Yendo, S. Arai, and T. Yamazato, "High performance demodulation method with less complexity for image-sensor communication," *Opt. Exp.*, vol. 27, no. 15, pp. 21565–21578, Jul. 2019.
[9] Z. Tang, S. Arai, T. Yendo, D. He, and T. Yamazato, "Sequential maximum likelihood decoding incorporating reliability determination for image sensor communication," *IEICE ComEX*, vol. 9, no. 8, pp. 365–370, Aug. 2020.

[10] T. Yamazato, "V2X communications with an image sensor," *J. Commun. Inf. Netw.*, vol. 2, no. 4, pp. 65–74, Dec. 2017.
[11] M. Kinoshita *et al.*, "Simplified vehicle vibration modeling for image sensor communication," *IEICE Trans. Fundamentals*, vol. 101-A, no. 1, pp. 176–184, Jan. 2018.
[12] C. Danakis, M. Afgani, G. Povey, I. Underwood, and H. Haas, "Using a CMOS camera sensor for visible light communication," in *Proc. IEEE Globecom Workshops*, 2012, pp. 1244–1248.
[13] Y. Imai, T. Ebihara, K. Mizutani, and N. Wakatsuki, "High-speed visible light communication using combination of low-speed image sensor and polygon mirror," *IEICE Trans. Fundamentals*, vol. E 99.A(1), no. 1, pp. 263–270, Jan. 2016.
[14] S. Arai, Z. Tang, A. Nakayama, H. Takada, and T. Yendo, "Implementation experiment of a rotary LED transmitter for improving the transmission rate for image sensor communication," in *Proc. IEEE Globecom Workshops*, 2020, pp. 1–6.
[15] S. Arai, Z. Tang, A. Nakayama, H. Takata, and T. Yendo, "Rotary LED transmitter for improving data transmission rate of image sensor communication," *IEEE Photon. J.*, vol. 13, no, 4, Aug. 2021, Art. no. 7300611.
[16] M. Alamouti, "A simple transmit diversity technique for wireless communications," *IEEE J. Sel. Areas Commun.*, vol. 16, no. 8, pp. 1451–1458, Oct. 1998.
[17] Y. Amano, K. Kamakura, and T. Yamazato, "Alamouti-type coding for visible light communication based on direct detection using image sensor," in *Proc. IEEE GLOBECOM*, 2013, pp. 2430–2435.
[18] W. H. Al-Natsheh, B. K. Hammad, and M. A. Abu Zaid, "Design and implementation of a cylindrical persistence of vision display," in *Proc. 6th Int. Conf. Elect. Electron. Eng.*, 2019, pp. 215–219.
[19] S. Golomb and G. Gong, *Signal Design for Good Correlation: For Wireless Communication, Cryptography, and Radar*. Cambridge, U.K.: Cambridge Univ. Press, 2005.
[20] *IEEE Standard for Local and Metropolitan Area Networks-Part 15 7: Short-Range Wireless Optical Communication Using Visible Light*, IEEE Standard 802.15.7-2011, Sep. 2011.